FULL PAPER

ADVANCED FUNCTIONAL MATERIALS

Quadratic Nonlinear Optical Properties of *N*-Aryl Stilbazolium Dyes**

By *Benjamin J. Coe,* James A. Harris, Inge Asselberghs, Koen Clays, Geert Olbrechts, André Persoons, Joseph T. Hupp, Robert C. Johnson, Simon J. Coles, Michael B. Hursthouse,* and *Keitaro Nakatani*

The new salts *trans*-4′-(dimethylamino)-*N*-R-4-stilbazolium hexafluorophosphate (R = methyl, Me **1**, phenyl, Ph **2**, 2,4-dinitrophenyl, DNPh **3**, 2-pyrimidyl, Pym **4**, Scheme 1) have been prepared. Their electronic absorption spectra show intense, visible intramolecular charge-transfer bands, the energy (E_{max}) of which decreases in the order R = Me > Ph > DNPh > Pym. This trend arises from the steadily increasing electron deficiency of the pyridinium ring, a phenomenon also observed in cyclic voltammetric and ^{1}H nuclear magnetic resonance (NMR) data. Fluorescence-free first hyperpolarizability β values of [**1**–**4**]PF_6 were measured by using femtosecond hyper-Rayleigh scattering (HRS) with acetonitrile solutions and a 1300 nm laser, and static first hyperpolarizabilities β_0 were obtained by application of the two-state model. The HRS results indicate that the *N*-aryl chromophores in [**2**–**4**]PF_6 have considerably larger β_0 values than their *N*-methyl counterpart in [**1**]PF_6, with a ca. 10-fold increase in β_0 observed in moving from [**1**]PF_6 to [**4**]PF_6 ($25 \rightarrow 230 \times 10^{-30}$ esu). Stark (electroabsorption) spectroscopic studies in butyronitrile glasses at 77 K allowed the derivation of dipole moment changes $\Delta\mu_{12}$ (10.9–14.8 D), which have been used to calculate β_0 according to the two-state equation $\beta_0 = 3\Delta\mu_{12}(\mu_{12})^2/2(E_{max})^2$ (μ_{12} = transition dipole moment). With the exception of [**1**]PF_6, the Stark-derived β_0 values are in reasonable agreement with those from HRS. However, the increase in β_0 in moving from [**1**]PF_6 to [**4**]PF_6 is only 2-fold for the Stark data ($90 \rightarrow 185 \times 10^{-30}$ esu). The observed trend of increasing β_0 in the order [**1**]PF_6 < [**3**]PF_6 < [**2**]PF_6 < [**4**]PF_6 arises from a combination of decreasing E_{max} and increasing $\Delta\mu_{12}$, with only a slight increase in μ_{12} between [**1**]PF_6 and [**4**]PF_6. It is likely that the β_0 values for [**3**]PF_6 are lower than expected due to the steric effect of the *ortho*-NO_2 group, which causes twisting of the DNPh ring out of the plane of the stilbazolium unit. A single crystal X-ray structure shows that [**2**]PF_6 crystallizes in the space group *Cc*, with head-to-tail alignment and almost parallel stacking of the pseudo-planar stilbazolium portions of the cations to form polar sheets within a polar bulk structure. [**2**]PF_6 is essentially isostructural with the related Schiff base salt *trans*-4-[(4-dimethylaminophenyl)iminomethyl]-*N*-phenylpyridinium hexafluorophosphate ([**8**]PF_6). Second harmonic generation (SHG) studies on [**2**]PF_6 and [**8**]PF_6 using a 1907 nm laser and sieved powdered samples (53–63 μm) afforded efficiencies of 470 and 240 times that of urea, respectively. Under the same conditions, the well-studied compound [**1**]*p*-$MeC_6H_4SO_3$ gave an SHG efficiency of 550 times that of urea.

[*] Dr. B. J. Coe, Dr. J. A. Harris
Department of Chemistry, University of Manchester
Oxford Road, Manchester M13 9PL (UK)
E-mail: b.coe@man.ac.uk

I. Asselberghs, Prof. K. Clays, G. Olbrechts, Prof. A. Persoons[+]
Laboratory of Chemical and Biological Dynamics
Center for Research on Molecular Electronics and Photonics
University of Leuven
Celestijnenlaan 200D, B-3001 Leuven (Belgium)

Prof. J. T. Hupp, R. C. Johnson
Department of Chemistry, Northwestern University
Evanston, IL 60208 (USA)

Dr. S. J. Coles, Prof. M. B. Hursthouse
EPSRC X-ray Crystallography Service
Department of Chemistry, University of Southampton
Highfield, Southampton SO17 1BJ (UK)

Prof. K. Nakatani
P.P.S.M., École Normale Supérieure de Cachan
URA 1906, avenue du Président Wilson, F-94235 Cachan (France)

[+] Second address: Optical Sciences Center, University of Arizona, Tucson, AZ 85721, USA.

[**] This work was supported by a studentship from the EPSRC (Dr. Harris), research grants from the Fund for Scientific Research-Flanders (FWO-V, G.0338.98 and G.0407.98), from the University of Leuven (GOA/95/01) and from the Belgian Government (IUAP P4/11), and sponsorship from the US Army Research Office MURI program.

1. Introduction

Molecular organic materials having nonlinear optical (NLO) properties are required for applications in emerging optoelectronic and photonic technologies.[1] NLO effects are useful because they allow the manipulation of laser beams, e.g., in frequency doubling or second harmonic generation (SHG), a quadratic effect. At the molecular level, quadratic NLO behavior is governed by first hyperpolarizabilities β, and static ("off-resonance") first hyperpolarizabilities β_0 are generally used when comparing active molecules. Amongst known NLO compounds, stilbazolium salts are particularly attractive for use in devices.[2]

Early studies showed that [**1**]*p*-$MeC_6H_4SO_3$ (DAST) exhibits pronounced bulk quadratic NLO activity, as evidenced by a powder SHG efficiency from a 1907 nm laser of ca. 10^3 times that of urea.[3] Also, a hyper-Rayleigh scattering (HRS) investigation of DAST using a 1064 nm laser afforded a very large β_0 value.[1c,4] Hence, DAST has been intensively investigated in recent years,[5] leading to the growth of large high-quality single crystals[6] and the fabrication of prototype NLO devices for parametric interactions and electro-optical (EO) modulation.[7]

  1616-301X/02/0202-0110 $ 17.50+.50/0

ADVANCED FUNCTIONAL MATERIALS

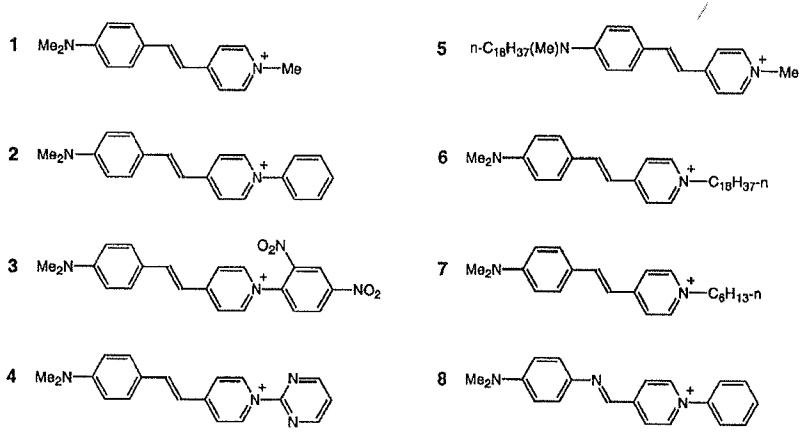

Scheme 1.

Stilbazolium chromophores have also been incorporated into various macroscopic structures such as Langmuir–Blodgett (LB) films,[8] intercalated layered materials,[9] self-assembled superlattices,[10] inclusion complexes[11] and guest–host[12] and side-chain polymer films.[13] Very recently, chiral stilbazolium salts of nickel bis(dithiolene) complex anions have been studied in attempts to combine quadratic NLO activity with semiconducting behavior,[14] and stilbazolium cations have been incorporated into SHG-active, ferromagnetic layered bimetallic networks.[15] Stilbazolium and related chromophores are also promising as two-photon absorption (a cubic NLO process) lasing dyes for converting infrared light into visible fluorescence.[16]

With the sole exception of a theoretical study on the neutral chromophore *trans*-4′-(dimethylamino)-*N*-(2-benzimidazolate)-4-stilbazolium,[17] only *N*-alkyl stilbazolium salts have been previously studied for their NLO properties. We have recently discovered that the β_0 values of dipolar ruthenium(II) ammine complexes of *N*-aryl pyridinium ligands are larger than those of their *N*-methyl analogues.[18] In these compounds the Ru^{II} centers act as electron donors and β_0 increases due to the greater electron-withdrawing abilities of *N*-aryl- with respect to *N*-methyl pyridinium groups. An analogous molecular engineering strategy should also enhance the quadratic NLO activities of purely organic pyridinium dyes such as stilbazolium salts.

2. Results and Discussion

2.1. Synthesis and Characterization

The known salt **[1]**I was prepared by the base-catalyzed condensation of *N*-methyl-4-picolinium iodide with 4-(dimethylamino)benzaldehyde,[19] and then metathesized to **[1]**PF_6 by precipitation from water/aqueous NH_4PF_6. The new cations *trans*-4′-(dimethylamino)-*N*-R-4-stilbazolium (R = phenyl **2**, 2,4-dinitrophenyl **3**, 2-pyrimidyl **4**) were prepared similarly by using the corresponding *N*-R-4-picolinium ions, and isolated as their PF_6^- salts.

The electronic absorption spectra of **[1–4]**PF_6 show intense, broad bands in the visible region (Table 1, Fig. 1), corresponding to intramolecular charge-transfer (ICT) excitations from the $-NMe_2$ electron donors to the pyridinium acceptors. The ICT band maximum energy E_{max} decreases in the order **[1]**PF_6 > **[2]**PF_6 > **[3]**PF_6 > **[4]**PF_6, with a difference of ca. 0.40 eV between the extremes. This trend is attributed to the steadily increasing electron deficiency of the pyridinium ring as the *N*-substituent changes from methyl to 2-pyrimidyl. This hypothesis is confirmed by cyclic voltammetric data (Table 1), which, although irreversible, show that the potential for oxidation of the $-NMe_2$ group remains constant, whilst that for reduction of the pyridinium unit becomes steadily less negative (and therefore reduction becomes easier) in the order **[1]**PF_6 < **[2]**PF_6 < **[4]**PF_6 < **[3]**PF_6. Also, the nuclear magnetic resonance (NMR) chemical shifts of the doublet signals for the

Table 1. Visible absorption, electrochemical, and ^1H NMR data for **[1–4]**PF_6 in acetonitrile.

Salt	λ_{max}[ICT] (ε) [a] [nm] ([M^{-1} cm^{-1}])	E_{max}[ICT] [eV]	E_{pa} [b] [V *vs.* Ag/AgCl] [e]	E_{pc} [c] [V *vs.* Ag/AgCl] [e]	$\delta[H^{2,6}]$ [d] [ppm]	$\delta[H^{3,5}]$ [d] [ppm]
[1]PF_6	470 (42 800)	2.64	0.94	−1.11	8.29	7.84
[2]PF_6	504 (51 400)	2.46	0.93	−0.88	8.57	7.98
[3]PF_6	537 (47 500)	2.31	0.96	−0.52	9.11	8.79
[4]PF_6	553 (57 200)	2.24	0.95	−0.66	9.53	9.01

[a] Solution concentrations ca. 10^{-5} M. [b] Peak potential for first irreversible oxidation (of highest occupied molecular orbital, HOMO, localized on $-NMe_2$ group); return wave also observed in some cases. [c] Peak potential for first irreversible reduction (of lowest unoccupied molecular orbital, LUMO, localized on pyridinium group); return wave also observed in some cases. [d] Signals for pyridinium ring protons; chemical shifts at 200 MHz with respect to TMS in CD_3CN. [e] Measured in solutions ca. 10^{-3} M in analyte and 0.1 M in $N^nBu_4PF_6$ at a platinum-disc working electrode with a scan rate of 200 mV s^{-1}. Ferrocene internal reference $E_{1/2}$ = 0.45 V.

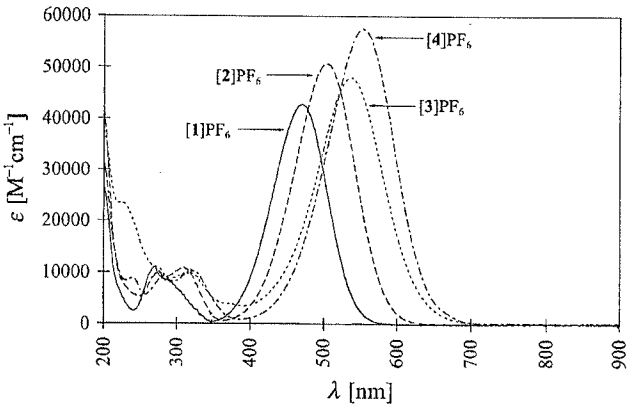

Fig. 1. Ultraviolet-visible (UV-vis) absorption spectra of the salts **[1–4]**PF_6 at RT in acetonitrile.

  1616-301X/02/0202-0111 $ 17.50+.50/0

protons of the pyridinium ring increase in the order [**1**]PF_6 < [**2**]PF_6 < [**3**]PF_6 < [**4**]PF_6, indicating decreasing shielding.

2.2. Hyper-Rayleigh Scattering Studies

The β values of [**1–4**]PF_6 were measured by using the HRS technique.[20] Because HRS usually overestimates β for molecules such as stilbazolium dyes, which show multi-photon fluorescence,[21] it is necessary to modify the experiment to obtain accurate data. Various approaches have been adopted in this context, such as simple subtraction of the fluorescence background,[22] the use of a 1907 nm laser,[23] and using a femtosecond laser to allow temporal discrimination between the HRS and fluorescence signals.[24] For [**1–4**]PF_6 we have used femtosecond HRS with a 1300 nm laser,[25] incorporating high-frequency demodulation of the fluorescence contributions.[26] This approach has previously been employed with *N*-alkyl stilbazolium salts,[11b,25,27] and has given good agreement with β_0 values for neutral chromophores from electric-field-induced SHG (EFISHG) studies.[28]

HRS β and β_0 values, obtained by application of the two-state model,[29] are presented in Table 2, together with literature data for several *N*-alkyl stilbazolium salts. Our HRS results indicate that the *N*-aryl chromophores in [**2–4**]PF_6 have considerably larger β_0 values than their *N*-methyl counterpart in [**1**]PF_6. Indeed, a ca. 10-fold increase in β_0 is observed in moving from [**1**]PF_6 to [**4**]PF_6. Although the β_0 for [**1**]PF_6 is much smaller than the value of 364×10^{-30} esu derived for DAST with a 1064 nm nanosecond laser,[1c,4] the latter result was heavily overestimated due to multiphoton fluorescence and the use of an inaccurate reference β value for the solvent.[21b] Nevertheless, the β_0 for [**1**]PF_6 is still relatively small when compared with those of [**5–7**]Br.[11b,25,27]

Table 2. Visible absorption and femtosecond HRS data for stilbazolium salts.

Salt	Solvent	λ_{max}[ICT] [nm]	β[a] [$\times 10^{30}$ esu]	β_0 [a]
[**1**]PF_6	CH_3CN	470	60	25
[**2**]PF_6	CH_3CN	504	355	120
[**3**]PF_6	CH_3CN	537	370	100
[**4**]PF_6	CH_3CN	553	1015	230
[**5**]Br [b]	$CHCl_3$	508	140	46
[**6**]Br [c]	$CHCl_3$	496	100	36
[**7**]Br [d]	$(CH_3)_2SO$	477	360	100

[a] β is the dynamic first hyperpolarizability measured using a 1300 nm laser fundamental for [**1–4**]PF_6 and [**5–6**]Br and a 800 nm laser fundamental for [**7**]Br; β_0 is the static first hyperpolarizability estimated by using the two-state model [29]. The quoted cgs units (esu) can be converted into SI units ($C^3 m^3 J^{-2}$) by dividing by a factor of 2.693×10^{20} (alternatively, conversion into units of $m^4 V^{-1}$ can be achieved by multiplying by a factor of 4.192×10^{-10}). [b] [25]. [c] [27]. [d] [11b].

The two-state model predicts that β_0 for a simple dipolar chromophore increases as the energy of the ICT band decreases, according to Equation 1:[29,30]

$$\beta_0 = \frac{3\Delta\mu_{12}(\mu_{12})^2}{2(E_{max})^2} \quad (1)$$

where $\Delta\mu_{12}$ is the dipole moment change between the ground and excited states and μ_{12} is the transition dipole moment. Even so, an E_{max} decrease of ca. 0.40 eV is clearly insufficient to explain the apparent 10-fold increase in β_0 in moving from [**1**]PF_6 to [**4**]PF_6.

2.3. Stark Spectroscopic Studies

In order to further investigate the molecular electronic properties of [**1–4**]PF_6, we have carried out Stark (electroabsorption) spectroscopic studies[31] to determine values of $\Delta\mu_{12}$. This technique has recently been applied to various compounds having quadratic NLO properties such as donor–acceptor polyenes,[32] porphyrins,[33] metallocenyl derivatives,[34] and Ru^{II} complexes.[35] The $|\Delta\mu_{12}|$ values obtained for [**1–4**]PF_6 are given in Table 3, together with oscillator strengths f_{os}, $|\mu_{12}|$ values and β_0 values calculated from Equation 1.

Table 3. Visible absorption and Stark spectroscopic data for [**1–4**]PF_6 at 77 K in butyronitrile.

Salt	λ_{max}[ICT] [nm]	E_{max}[ICT] [eV]	f_{os} [a]	$\lvert\mu_{12}\rvert$ [b] [D]	$\lvert\Delta\mu_{12}\rvert$ [D]	β_0 [c] [10^{-30} esu]
[**1**]PF_6	483	2.57	0.90	9.6	10.9	90
[**2**]PF_6	515	2.41	1.02	10.6	12.0	135
[**3**]PF_6	528	2.35	0.82	9.6	13.3	130
[**4**]PF_6	565	2.19	0.88	10.1	14.8	185

[a] Oscillator strength obtained from $(4.32 \times 10^{-9}$ M cm$^2)$ A, where A is the integrated extinction coeffiecient. [b] Transition dipole moment calculated by using Equation 3. [c] Static first hyperpolarizability calculated by using Equation 1.

With the exception of [**1**]PF_6, the β_0 values derived from the Stark measurements are in reasonable agreement with those from femtosecond HRS. However, the increase in β_0 in moving from [**1**]PF_6 to [**4**]PF_6 is only 2-fold for the Stark data, as opposed to 10-fold with the HRS values. This large difference can be traced primarily to the small HRS β_0 value for [**1**]PF_6. In any case, the Stark data do confirm that β_0 increases in the order [**1**]PF_6 < [**3**]PF_6 ≤ [**2**]PF_6 < [**4**]PF_6. Furthermore, this trend arises from a combination of decreasing E_{max} and increasing $\Delta\mu_{12}$, with only a slight increase in μ_{12} between [**1**]PF_6 and [**4**]PF_6. It is likely that the β_0 values for [**3**]PF_6 are lower than expected due to the steric effect of the *ortho*-NO_2 group, which causes twisting of the 2,4-dinitrophenyl ring out of the plane of the stilbazolium unit. By contrast, in [**2**]PF_6 and [**4**]PF_6 the *N*-aryl rings are more likely to exist coplanar with the stilbazolium units, leading to larger β_0 values. A similar effect has previously been observed in the complex $[Ru^{II}(NH_3)_5(2,4\text{-DNPhQ}^+)]^{3+}$ [2,4-DNPhQ$^+$ = *N*-(2,4-dinitrophenyl)-4,4′-bipyridinium], which has a lower metal-to-ligand charge-transfer energy, but a similar β_0, compared with its *N*-phenyl analogue.[18a]

At present it is not possible to state categorically which β_0 values determined for [**1–4**]PF_6 are the more reliable. However, the close agreement between the Stark and HRS values for [**2–4**]PF_6 suggests that it is one of the β_0 values for [**1**]PF_6 that is most likely to be less reliable. Additional comparative experiments must be carried out before this point can be commented on further. It is noteworthy that very few previous

1616-301X/02/0202-0112 $ 17.50+.50/0

studies have attempted to compare β_0 values obtained via both HRS and Stark measurements, and none have done so for stilbazolium chromophores. In any case, the agreement between the Stark and HRS β_0 values for [**2**–**4**]PF_6 provides empirical confirmation that the two-state model is reasonably appropriate for stilbazolium chromophores.

2.4. X-ray Crystallographic Study

In order for a compound to exhibit macroscopic quadratic NLO effects, the active molecules must be arranged non-centrosymmetrically.[1] The marked NLO properties of DAST crystals arise from a favorable orientation of the dipolar cations in the *Cc* space group. We have obtained a single crystal X-ray structure of [**2**]PF_6; a representation of the molecular structure is shown in Figure 2 and a packing diagram in Figure 3. The small dihedral angle of 10.8(2)° between the pyridyl and phenylene rings[36] is consistent with π-electronic coupling through the stilbazolium framework. The phenyl substituent is twisted with respect to the pyridyl ring,[36] giving a dihedral angle of 55.8(1)°. As expected, the cation in [**2**]PF_6 shows some degree of ground-state charge-separation. For example, the stilbazolium rings are partially quinoidal: the average of the distances C7–C8 and C10–C11 is ca. 0.05 Å less than the average of C8–C9 and C9–C10, and the average of C15–C16 and C18–C19 is ca. 0.03 Å less than the average of the other C–C distances within the phenyl ring.

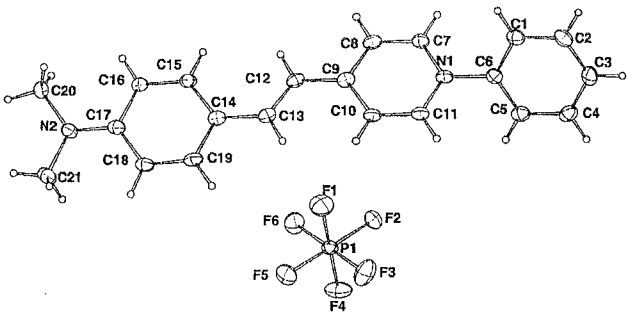

Fig. 2. Structural representation of the salt [**2**]PF_6 (50 % probability ellipsoids). Selected interatomic distances [Å] and angles [°]: N1–C7 1.363(3), N1–C11 1.370(3), N1–C6 1.436(3), N2–C17 1.360(3), C7–C8 1.360(4), C8–C9 1.407(4), C9–C10 1.405(3), C9–C12 1.435(4), C10–C11 1.353(4), C12–C13 1.363(4), C13–C14 1.433(4), C14–C19 1.400(4), C14–C15 1.406(4), C15–C16 1.370(4), C16–C17 1.427(4), C17–C18 1.402(4). C18–C19 1.384(4); C7–N1–C6 121.6(2), C11–N1–C6 119.2(2), C10–C9–C12 123.4(2), C8–C9–C12 120.4(2), C13–C12–C9 124.5(2), C12–C13–C14 126.9(3), C19–C14–C13 119.8(3), C15–C14–C13 123.7(3), N2–C17–C18 122.7(2), N2–C17–C16 120.4(3).

Although the presence of *para*-toluenesulfonate anions generally appears to encourage stilbazolium cations to pack non-centrosymmetrically,[19] [**2**]PF_6 also crystallizes in *Cc*, and is essentially isostructural with the related Schiff base [**8**]PF_6.[37] The pseudo-planar stilbazolium portions of the cations of [**2**]PF_6 align head-to-tail and stack almost parallel, forming polar sheets within a polar bulk structure (Fig. 3). The PF_6^- anions lie in between the cationic sheets, located close to the electron-deficient pyridinium rings. Similar packing structures are observed in DAST and related compounds, in which it has been suggested that the intervening anions act to reduce dipole–dipole interactions, which would otherwise cause antiparallel alignment of the polar cationic sheets.[3,19]

2.5. Kurtz Powder Test Studies

As a preliminary test of their bulk NLO activities, we have carried out powder SHG studies on [**2**]PF_6 and [**8**]PF_6 using a 1907 nm laser fundamental to avoid absorption of the harmonic signals. Unsized microcrystalline samples gave SHG efficiencies of 600 and 400 times that of a urea reference, for [**2**]PF_6 and [**8**]PF_6, respectively. The SHG activity of DAST is amongst the largest of any known material, and comparison with [**2**]PF_6 and [**8**]PF_6 is of great interest. Using sieved powdered samples (53–63 μm), we obtained SHG efficiencies of 470, 240, and 550 times that of urea for [**2**]PF_6, [**8**]PF_6, and DAST, respectively. It can hence be concluded that our new salts show very high SHG activities, that of [**2**]PF_6 comparing favorably with that of DAST. Since [**2**]PF_6 and [**8**]PF_6 are isostructural,[37] it is likely that the consistently lower SHG efficiency of the latter is largely a result of the β_0 of $[\mathbf{8}]^+$ being smaller than that of $[\mathbf{2}]^+$. Previous EFISHG studies have established that azomethine substitutions in stilbenyl bridges lead to large decreases in β_0.[38]

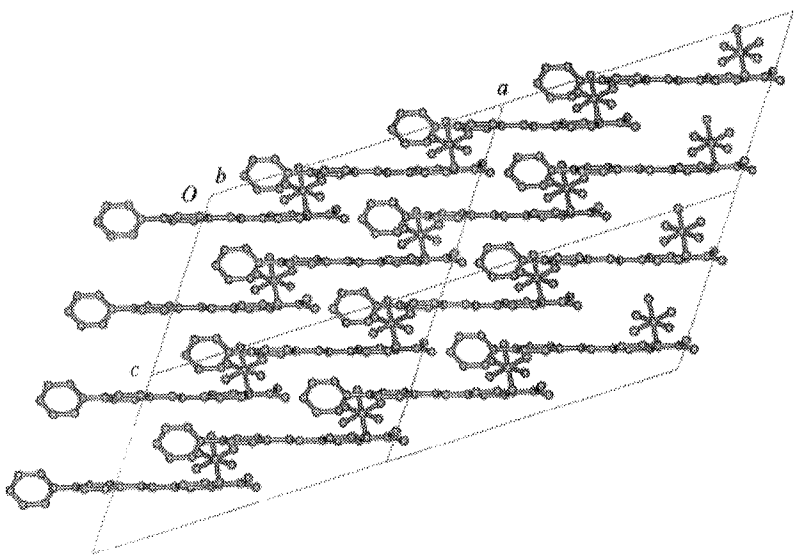

Fig. 3. Crystal packing diagram of [**2**]PF_6 (viewed along the *b*-axis).

In [**2**]PF_6, the angle θ_m between the dipolar axis (approximated as the N1–N2 vector) and the crystallographic *b*-axis is 74.5(1)°, which can be compared with the optimal θ_m value for SHG phase-matching in the *m* symmetry point group of 35.26°.[39] The structure of [**2**]PF_6 is hence not optimized for SHG, but is better suited for EO behavior, which ideally

  1616-301X/02/0202-0113 $ 17.50+.50/0

requires completely parallel alignment of molecular dipoles.[1] As in DAST,[19] the angle between the dipolar axis and the crystallographic *a*-axis in [**2**]PF_6 is ca. 20°. Given the larger β_0 value for [**2**]$^+$ with respect to [**1**]$^+$, it can hence be anticipated that crystals of [**2**]PF_6 may exhibit larger EO coefficients than those of DAST. Preliminary crystal growing experiments have provided encouraging results. Crystals of [**2**]PF_6 having a minimum dimension of ca. 1 mm and a maximum dimension of ca. 5 mm have already been grown simply by slow evaporation of acetonitrile solutions, and larger crystals should be attainable without undue problems. Furthermore, given that [**4**]PF_6 has a substantially larger β_0 than [**1**]PF_6, the incorporation of [**4**]$^+$ into appropriate macroscopic structures is an attractive strategy for further enhancing bulk NLO properties. The most obvious way to achieve this objective would be to grow crystals of various counter-anions in the hope of obtaining non-centrosymmetric packing arrangements. Alternatively, 5-alkyl-2-chloropyrimidines[40] could be used to prepare derivatives of [**4**]$^+$ suitable for LB film formation.

3. Conclusions

Femtosecond HRS measurements have been used to obtain fluorescence-free β_0 values for a known *N*-alkyl and three new *N*-aryl stilbazolium cations. Stark spectroscopy has also been applied for the first time to such compounds, providing confirmation and rationalization of the observation that the *N*-aryl chromophores have considerably larger β_0 values than their *N*-methyl analogue. This study represents the first instance in which a molecular engineering approach has been used to enhance the NLO responses of stilbazolium cations, and a similar strategy should be applicable to other pyridinium-based chromophores. The synthetic simplicity of *N*-arylation renders this approach particularly attractive and versatile. In addition, [**2**]PF_6 crystallizes non-centrosymmetrically and shows pronounced SHG activity, which is similar to that of DAST. The novel chromophores [**2–4**]$^+$ will be readily incorporated into various crystalline salts or derivatized to allow the fabrication of macroscopic structures such as LB films, which can be expected to show pronounced bulk NLO effects.

4. Experimental

General: ^{1}H NMR spectra were recorded on a Varian Gemini 200 spectrometer and all shifts are referenced to tetramethylsilane (TMS). The fine splitting of pyridyl or phenyl ring AA′BB′ patterns is ignored and the signals are reported as simple doublets, with *J* values referring to the two most intense peaks. Electronic absorption spectra were recorded by using a Varian Cary 1E spectrophotometer and elemental analyses were performed by the Microanalytical Laboratory, University of Manchester. Cyclic voltammetric measurements were carried out by using an EG&G PAR model 173 potentiostat/galvanostat with a model 175 universal programmer. An EG&G PAR K0264 single-compartment microcell was used with a Ag/AgCl reference electrode (3 M NaCl, saturated AgCl), a platinum-disc working electrode, and platinum-wire auxiliary electrode. Acetonitrile (high-pressure liquid chromatography, HPLC, grade) was used as received and tetra-*n*-butyl ammonium hexafluorophosphate, twice recrystallized from ethanol and dried in vacuo, as supporting electrolyte. Solutions containing ca. 10^{-3} mol dm^{-3} analyte (0.1 mol dm^{-3} electrolyte) were deaerated by purging with N_2. All $E_{1/2}$ values were calculated from $(E_{pa} + E_{pc})/2$ at a scan rate of 200 mV s^{-1}.

Materials: All reagents were purchased from Lancaster Synthesis, Acros, and Aldrich and used without further purification. The products were dried overnight at room temperature (RT) in a vacuum desiccator ($CaSO_4$) prior to characterization.

N-(2,4-Dinitrophenyl)-4-picolinium Hexafluorophosphate, [dnppic$^+$]PF$_6$: A solution of 4-picoline (2.4 mL, 25 mmol) and 2,4-dinitrochlorobenzene (5.00 g, 25 mmol) in ethanol (25 mL) was heated under reflux for 2 h. After cooling to RT, diethyl ether was added and the black precipitate was filtered off, washed with diethyl ether and dried. The crude product was purified by precipitation from boiling ethanol/diethyl ether. The resulting gray solid was filtered off, washed with diethyl ether and dried to afford crude [dnppic$^+$]Cl [5.18 g. ^{1}H NMR (200 MHz, D_2O): δ = 9.31 (d, 1H, *J* = 2.5 Hz, H^3), 8.89–8.83 (m, 3H, H^5 + C_5H_4N), 8.19–8.06 (m, 3H, H^6 + C_5H_4N), 2.79 (s, 3H, Me)]. This material is unstable in air and was hence not further purified, but was dissolved in a minimum volume of water and aqueous NH_4PF_6 was added. The precipitate was filtered off, washed with water, and dried. Further purification was effected by precipitation from acetone/diethyl ether; yield: 5.38 g (53 %). ^{1}H NMR (200 MHz, CD_3COCD_3): δ = 9.27–9.24 (m, 3H, C_5H_4N + H^3), 9.01 (dd, 1H, *J* = 2.5, 8.7 Hz, H^5), 8.54 (d, 1H, *J* = 8.8 Hz, H^6), 8.39 (d, 2H, *J* = 6.5 Hz, C_5H_4N), 2.94 (s, 3H, Me). C,H,N analysis calcd. for $C_{12}H_{10}F_6N_3O_4P$: C 35.57, H 2.49, N 10.37; found: C 35.68, H 2.56, N 10.46.

N-Phenyl-4-picolinium Chloride, [ppic$^+$]Cl: A sample of [dnppic$^+$]Cl, prepared as described above, was dissolved in boiling ethanol (30 mL), aniline (5.6 mL, 61 mmol) was added and the resulting solution was heated under reflux for 3 h. The solution was cooled to RT and reduced to half volume in vacuo. The addition of water caused formation of a green precipitate, which was filtered off, washed with water, and discarded. The filtrate was reduced to dryness and dissolved in ethanol. The addition of diethyl ether afforded a golden-brown precipitate which was filtered off, washed with diethyl ether, and dried; yield: 2.24 g (39 %). ^{1}H NMR (200 MHz, D_2O): δ = 8.85 (d, 2H, *J* = 6.6 Hz, C_5H_4N), 7.99 (d, 2H, *J* = 6.9 Hz, C_5H_4N), 7.67 (s, 5H, Ph), 2.71 (s, 3H, Me). C,H,N analysis calcd. for $C_{12}H_{12}ClN{\cdot}1.25H_2O$: C 63.16, H 6.40, N 6.14; found: C 63.30, H 6.06, N 6.23.

N-(2-Pyrimidyl)-4-picolinium Hexafluorophosphate, [pympic$^+$]PF$_6$: A mixture of 2-chloropyrimidine (2.86 g, 25 mmol) and 4-picoline (1.2 mL, 12.5 mmol) was heated to produce a dark green solution. Ethanol (5 mL) was added and the resulting solution was heated under reflux for 8 h. After cooling to RT, the addition of diethyl ether afforded a gray/green precipitate, which was filtered off, washed with diethyl ether, and dried; yield: 1.16 g. ^{1}H NMR (200 MHz, D_2O): δ = 9.76 (d, 2H, *J* = 6.6 Hz, C_5H_4N), 9.04 (d, 2H, *J* = 4.9 Hz, $C_4N_2H_3$), 8.07 (d, 2H, *J* = 6.6 Hz, C_5H_4N), 7.79 (t, 1H, *J* = 4.9 Hz, $C_4N_2H_3$), 2.75 (s, 3H, Me). This material was dissolved in a minimum volume of water and aqueous NH_4PF_6 was added. A black precipitate was filtered off and discarded. Further addition of aqueous NH_4PF_6 yielded a yellow precipitate, which was filtered off, washed with water, and dried. Purification was effected by precipitation from acetone/diethyl ether; yield: 1.64 g (41 %). ^{1}H NMR (200 MHz, CD_3COCD_3): δ = 10.08 (d, 2H, *J* = 7.0 Hz, C_5H_4N), 9.23 (d, 2H, *J* = 4.8 Hz, $C_4N_2H_3$), 8.35 (d, 2H, *J* = 6.9 Hz, C_5H_4N), 7.98 (t, 1H, *J* = 4.9 Hz, $C_4N_2H_3$), 2.92 (s, 3H, Me). C,H,N analysis calcd. for $C_{10}H_{10}F_6N_3P{\cdot}0.06C_4H_{10}O$: C 38.24, H 3.32, N 13.07; found: C 38.33, H 3.24, N 13.07.

Trans-4′-(Dimethylamino)-N-methyl-4-stilbazolium Hexafluorophosphate, [1]PF$_6$: ^{1}H NMR (200 MHz, CD_3CN): δ = 8.29 (d, 2H, *J* = 6.9 Hz, C_5H_4N), 7.84 (d, 2H, *J* = 6.8 Hz, C_5H_4N), 7.86 (d, 1H, *J* = 15.9 Hz, CH), 7.59 (d, 2H, *J* = 8.9 Hz, C_6H_4), 7.06 (d, 1H, *J* = 15.8 Hz, CH), 6.80 (d, 2H, *J* = 8.9 Hz, C_6H_4), 4.12 (s, 3H, N^+–Me), 3.08 (s, 6 H, NMe_2). C,H,N analysis calcd. for $C_{16}H_{19}F_6N_2P$: C 50.01, H 4.98, N 7.29; found: C 50.10, H 4.92, N 7.29.

Trans-4′-(Dimethylamino)-N-phenyl-4-stilbazolium Hexafluorophosphate, [2]PF$_6$: A solution of [ppic$^+$]Cl·1.25H_2O (250 mg, 1.10 mmol), 4-(dimethylamino)benzaldehyde (363 mg, 2.4 mmol), and piperidine (4 drops) in methanol (20 mL) was heated under reflux for 4 h. The addition of diethyl ether to the deep red solution afforded a dark precipitate, which was filtered off, washed with diethyl ether, and dried (390 mg). This crude chloride salt was metathesized to [**2**]PF_6 by precipitation from water/aqueous NH_4PF_6; yield: 468 mg (96 %). ^{1}H NMR (200 MHz, CD_3CN): δ = 8.57 (d, 2H, *J* = 7.0 Hz, C_5H_4N), 7.98 (d, 2H, *J* = 7.0 Hz, C_5H_4N), 7.91 (d, 1H, *J* = 15.9 Hz, CH), 7.70 (s, 5H, Ph), 7.65 (d, 2H, *J* = 9.1 Hz, C_6H_4), 7.15 (d, 1H, *J* = 15.8 Hz, CH), 6.82 (d, 2H, *J* = 8.9 Hz, C_6H_4), 3.08 (s, 6H, NMe_2). C,H,N analysis calcd. for $C_{21}H_{21}F_6N_2P$: C 56.51, H 4.74, N 6.28; found: C 56.35, H 5.04, N 6.11. Diffraction quality crystals were grown by slow evaporation of an acetonitrile solution at RT.

Trans-4′-(Dimethylamino)-N-(2,4-dinitrophenyl)-4-stilbazolium Hexafluorophosphate, [3]PF$_6$: A solution of [dnppic$^+$]PF_6 (196 mg, 0.48 mmol), 4-(dimethylamino)benzaldehyde (149 mg, 1.0 mmol), and piperidine (2 drops) in methanol (20 mL) was heated under reflux for 4 h. The addition of diethyl ether to the deep purple solution afforded a dark precipitate, which was filtered off, washed with diethyl ether, and dried; yield: 127 mg (50 %). ^{1}H NMR (200 MHz, CD_3CN): δ = 9.11 (d, 1H, *J* = 2.5 Hz, H^3), 8.79 (dd, 1H, *J* = 8.7, 2.5 Hz, H^5), 8.39 (d, 2H, *J* = 7.1 Hz, C_5H_4N), 8.08 (d, 1H, *J* = 8.7 Hz, H^6), 7.99 (d, 1H, *J* = 15.8 Hz, CH), 7.98 (d, 2H, *J* = 7.2 Hz, C_5H_4N), 7.68 (d, 2H, *J* = 9.1 Hz, C_6H_4), 7.17 (d, 1H, *J* = 15.8 Hz, CH), 6.83 (d, 2H, *J* = 9.0 Hz, C_6H_4), 3.11 (s, 6H, NMe_2). C,H,N anal-

  1616-301X/02/0202-0114 $ 17.50+.50/0

ysis calcd. for $C_{21}H_{19}F_6N_4O_4P$: C 47.03, H 3.57, N 10.45; found: C 47.02, H 3.71, N 10.40.

Trans-4′-(Dimethylamino)-N-(2-pyrimidyl)-4-stilbazolium Hexafluorophosphate, [4]PF$_6$: This was prepared and purified in identical fashion to **[2]**PF_6 by using [pympic$^+$]PF_6·0.06$C_4H_{10}O$ (161 mg, 0.50 mmol) and 4-(dimethylamino)-benzaldehyde (149 mg, 1.0 mmol). A purple solid was obtained; yield: 72 mg (32 %). ^{1}H NMR (200 MHz, CD_3CN): δ = 9.53 (d, 2H, J = 7.4 Hz, C_5H_4N), 9.01 (d, 2H, J = 4.8 Hz, $C_4N_2H_3$), 8.00 (d, 1H, J = 16.0 Hz, CH), 7.97 (d, 2H, J = 7.5 Hz, C_5H_4N), 7.71 (t, 1H, J = 4.8 Hz, $C_4N_2H_3$), 7.68 (d, 2H, J = 9.0 Hz, C_6H_4), 7.19 (d, 1H, J = 15.8 Hz, CH), 6.82 (d, 2H, J = 9.1 Hz, C_6H_4), 3.10 (s, 6H, NMe_2). C,H,N analysis calcd. for $C_{19}H_{19}F_6N_4P$: C 50.90, H 4.27, N 12.50; found: C 51.15, H 4.29, N 12.78.

Crystal Data for [2]PF$_6$: $C_{21}H_{21}F_6N_2P$, M_r = 446.37, monoclinic, space group *Cc*, a = 19.384(4), b = 10.636(2), c = 11.784(2) Å, β = 125.93(3)°, V = 1967.3(7) Å^3, ρ_{calcd} = 1.507 Mg m^{-3}, T (K) = 150(2), Z = 4, μ = 0.206 mm^{-1} (Mo Kα); red plate 0.55 × 0.17 × 0.04 mm^3; 8007 reflections collected, 3783 independent reflections (R_{int} = 0.0573), $2\theta_{max}$ = 54.96°. Data were collected on a Nonius Kappa charge coupled device (CCD) area-detector diffractometer controlled by the Collect software package [41]. Images were processed by Denzo [42] and the data were corrected for absorption by using the empirical method employed in Sortav [43]. The structure was solved by direct methods and refined by full-matrix least-squares against all F_0^2 data using SHELX-97 [44], which gave wR_2 = 0.1009 and R_1 = 0.0420 for $I > 2\sigma(I)$ [S = 1.027; 275 parameters; peak and hole = 0.263, –0.268 e Å^{-3}; all non-hydrogen atoms anisotropic]. Crystallographic data (excluding structure factors) for the structure reported in this paper have been deposited with the Cambridge Crystallographic Data Center as supplementary publication no. CCDC-163560. Copies of the data can be obtained, free of charge, on application to CCDC, 12 Union Road, Cambridge CB2 1EZ, UK (fax: (+44) 1223-336-033; e-mail: deposit@ccdc.cam.ac.uk).

Hyper-Rayleigh Scattering: The apparatus and experimental procedure were exactly as described previously [25–27]. β values were determined by using β_{1300} for disperse red 1 (86 × 10^{-30} esu in acetonitrile: obtained from the value of 54 × 10^{-30} esu in $CHCl_3$ and taking into account local field correction factors at optical frequencies) as an external reference.

Stark Spectroscopy: The apparatus used for performing the Stark measurements has been described previously [45], and butyronitrile was used as the glassing medium. The electroabsorption (ΔA) signals were fit using Equation 2 [46], where $A(\nu)$ is the unperturbed ("field off") absorption spectrum, F_{int} is the internal electric field, h is Planck's constant, and c is the speed of light.

$$\Delta A(\nu) = \left\{ A_\chi A(\nu) + \frac{B_\chi \nu}{15hc} \frac{d[A(\nu)/\nu]}{d\nu} + \frac{C_\chi \nu}{30h^2c^2} \frac{d^2[A(\nu)/\nu]}{d\nu^2} \right\} F_{int}^2 \quad (2)$$

F_{int} is approximated by 1.3 × $F_{applied}$ to correct for local field effects due to the dielectric constant of the solvent glass. Neglecting cross terms, A_χ is proportional to the transition moment polarizability and hyperpolarizability, B_χ describes changes in polarizability, and C_χ gives the absolute value of the dipole moment change. The C_χ (second derivative) component is typically dominant for ICT transitions and is often readily evident in the lineshape of the Stark spectrum. The C_χ contribution was dominant for **[1–4]**PF_6, and in all cases excellent fits to Equation 2 were found. Values of $|\mu_{12}|$ were derived from Equation 3, where f_{os} is the oscillator strength of the ICT absorption:

$$|\mu_{12}| = [f_{os}/(1.08 \times 10^{-5}(E_{max}))]^{1/2} \quad (3)$$

SHG Measurements: These were carried out at RT using the Kurtz–Perry powder technique [47]. The 1.064 μm fundamental from a ps Nd:YAG pulsed (10 Hz) laser was passed through a 1 m long hydrogen cell under a pressure of 50 bar to generate the 1.907 μm beam. The samples consisted of microcrystalline powders unsized or sieved to a particle size distribution of 53–63 μm and squeezed between two glass plates with a sheet of spacer between to give an approximately constant sample thickness. After passing through appropriate filters, the transmitted signals were detected by a photomultiplier and visualized on an ultrafast Tektronix 7834 oscilloscope. The SHG signals were calibrated with respect to unsized or 53–63 μm powdered urea samples.

Received: October 5, 2001

[1] a) *Nonlinear Optical Properties of Organic Molecules and Crystals*, Vol. 1–2 (Eds: D. S. Chemla, J. Zyss), Academic, New York **1987**. b) C. Bosshard, K. Sutter, P. Prêtre, J. Hulliger, M. Flörsheimer, P. Kaatz, P. Günter, *Organic Nonlinear Optical Materials, Advances in Nonlinear Optics*, Vol. 1, Gordon and Breach, Amsterdam **1995**. c) T. Verbiest, S. Houbrechts, M. Kauranen, K. Clays, A. Persoons, *J. Mater. Chem.* **1997**, *7*, 2175. d) *Nonlinear Optics of Organic Molecules and Polymers* (Eds: H. S. Nalwa, S. Miyata), CRC Press, Boca Raton, FL **1997**.

[2] K.-S. Lee, O.-K. Kim, *Photonics Sci. News* **1999**, *4*, 9.

[3] S. R. Marder, J. W. Perry, W. P. Schaefer, *Science* **1989**, *245*, 626.

[4] X.-M. Duan, S. Okada, H. Oikawa, H. Matsuda, H. Nakanishi, *Mol. Cryst. Liq. Cryst.* **1995**, *267*, 89.

[5] U. Meier, M. Bösch, C. Bosshard, P. Günter, *Synth. Met.* **2000**, *109*, 19.

[6] a) F. Pan, M. S. Wong, C. Bosshard, P. Günter, *Adv. Mater.* **1996**, *8*, 592. b) H. Adachi, Y. Takahashi, J. Yabuzaki, Y. Mori, T. Sasaki, *J. Cryst. Growth* **1999**, *199*, 568. c) S. Sohma, H. Takahashi, T. Taniuchi, H. Ito, *Chem. Phys.* **1999**, *245*, 359.

[7] a) F. Pan, G. Knöpfle, C. Bosshard, S. Follonier, R. Spreiter, M. S. Wong, P. Günter, *Appl. Phys. Lett.* **1996**, *69*, 13. b) U. Meier, M. Bösch, C. Bosshard, F. Pan, P. Günter, *J. Appl. Phys.* **1998**, *83*, 3486. c) M. Thakur, J. J. Xu, A. Bhowmik, L. G. Zhou, *Appl. Phys. Lett.* **1999**, *74*, 635. d) F. Pan, K. McCallion, M. Chiapetta, *Appl. Phys. Lett.* **1999**, *74*, 492. e) A. K. Bhowmik, S. Tan, A. C. Ahyi, A. Mishra, M. Thakur, *Polym. Mater. Sci. Eng.* **2000**, *83*, 169.

[8] a) G. J. Ashwell, in *Organic Materials for Non Linear Optics III* (Eds: G. J. Ashwell, D. Bloor), Royal Society of Chemistry, Cambridge **1993**. b) G. J. Ashwell, R. C. Hargreaves, C. E. Baldwin, G. S. Bahra, C. R. Brown, *Nature* **1992**, *357*, 393. c) P. Hodge, Z. Ali-Adib, D. West, T. A. King, *Thin Solid Films* **1994**, *244*, 1007. d) J. H. Xu, X. Z. Lu, G. P. Zhou, Z. M. Zhang, *Thin Solid Films* **1998**, *312*, 295.

[9] a) P. G. Lacroix, R. Clément, K. Nakatani, J. Zyss, I. Ledoux, *Science* **1994**, *263*, 658. b) T. Coradin, R. Clément, P. G. Lacroix, K. Nakatani, *Chem. Mater.* **1996**, *8*, 2153.

[10] a) D. Li, M. A. Ratner, T. J. Marks, C. Zhang, J. Yang, G. K. Wong, *J. Am. Chem. Soc.* **1990**, *112*, 7389. b) S. Yitzchaik, T. J. Marks, *Acc. Chem. Res.* **1996**, *29*, 197.

[11] a) O.-K. Kim, L.-S. Choi, H.-Y. Zhang, X. H. He, Y.-H. Shih, *J. Am. Chem. Soc.* **1996**, *118*, 12220. b) K. Clays, G. Olbrechts, T. Munters, A. Persoons, O.-K. Kim, L.-S. Choi, *Chem. Phys. Lett.* **1998**, *293*, 337.

[12] I. Liakatas, M. S. Wong, C. Bosshard, M. Ehrensperger, P. Günter, *Ferroelectrics* **1997**, *202*, 299.

[13] N. Nemoto, J. Abe, F. Miyata, Y. Shirai, Y. Nagase, *J. Mater. Chem.* **1997**, *7*, 1389.

[14] R. Andreu, I. Malfant, P. G. Lacroix, H. Gornitzka, K. Nakatani, *Chem. Mater.* **1999**, *11*, 840.

[15] S. Bénard, P. Yu, J. P. Audière, E. Rivière, R. Clément, J. Guilhem, L. Tchertanov, K. Nakatani, *J. Am. Chem. Soc.* **2000**, *122*, 9444.

[16] a) G. S. He, L. Yuan, Y. Cui, M. Li, P. N. Prasad, *J. Appl. Phys.* **1997**, *81*, 2529. b) A. Abbotto, L. Beverina, R. Bozio, S. Bradamante, C. Ferrante, G. A. Pagani, R. Signorini, *Adv. Mater.* **2000**, *12*, 1963.

[17] J. Abe, Y. Shirai, N. Nemoto, Y. Nagase, *J. Phys. Chem. B* **1997**, *101*, 1910.

[18] a) B. J. Coe, J. A. Harris, L. J. Harrington, J. C. Jeffery, L. H. Rees, S. Houbrechts, A. Persoons, *Inorg. Chem.* **1998**, *37*, 3391. b) B. J. Coe, J. A. Harris, I. Asselberghs, A. Persoons, J. C. Jeffery, L. H. Rees, T. Gelbrich, M. B. Hursthouse, *J. Chem. Soc., Dalton Trans.* **1999**, 3617.

[19] S. R. Marder, J. W. Perry, C. P. Yakymyshyn, *Chem. Mater.* **1994**, *6*, 1137.

[20] a) R. W. Terhune, P. D. Maker, C. M. Savage, *Phys. Rev. Lett.* **1965**, *14*, 681. b) K. Clays, A. Persoons, *Phys. Rev. Lett.* **1991**, *66*, 2980. c) K. Clays, A. Persoons, *Rev. Sci. Instrum.* **1992**, *63*, 3285. d) K. Clays, A. Persoons, L. De Maeyer, in *Modern Nonlinear Optics*, Vol. 3 (Eds: M. Evans, S. Kielich), Wiley, New York **1994**. e) E. Hendrickx, K. Clays, A. Persoons, *Acc. Chem. Res.* **1998**, *31*, 675.

[21] a) M. C. Flipse, R. de Jonge, R. H. Woudenberg, A. W. Marsman, C. A. van Walree, L. W. Jenneskens, *Chem. Phys. Lett.* **1995**, *245*, 297. b) I. D. Morrison, R. G. Denning, W. M. Laidlaw, M. A. Stammers, *Rev. Sci. Instrum.* **1996**, *67*, 1445. c) S. Stadler, G. Bourhill, C. Bräuchle, *J. Phys. Chem.* **1996**, *100*, 6927.

[22] N. W. Song, T.-I. Kang, S. C. Jeoung, S.-J. Jeon, B. R. Cho, D. Kim, *Chem. Phys. Lett.* **1996**, *261*, 307.

[23] M. A. Pauley, C. H. Wang, *Chem. Phys. Lett.* **1997**, *280*, 544. *Rev. Sci. Instrum.* **1999**, *70*, 1277.

[24] O. F. J. Noordman, N. F. van Hulst, *Chem. Phys. Lett.* **1996**, *253*, 145.

[25] G. Olbrechts, K. Wostyn, K. Clays, A. Persoons, *Opt. Lett.* **1999**, *24*, 403.

[26] G. Olbrechts, R. Strobbe, K. Clays, A. Persoons, *Rev. Sci. Instrum.* **1998**, *69*, 2233.

[27] K. Clays, K. Wostyn, G. Olbrechts, A. Persoons, A. Watanabe, K. Nogi, X.-M. Duan, S. Okada, H. Oikawa, H. Nakanishi, H. Vogel, D. Beljonne, J.-L. Brédas, *J. Opt. Soc. Am. B* **2000**, *17*, 256.

[28] For example, the β_0 of 53 × 10^{-30} esu [25] obtained for *trans*-4′-(dimethylamino)-4-nitrostilbene compares with an EFISHG value of 55 × 10^{-30} esu (data in $CHCl_3$; L.-T. Cheng, W. Tam, S. R. Marder, A. E. Stiegman, G. Rikken, C. W. Spangler, *J. Phys. Chem.* **1991**, *95*, 10643).

[29] a) J. L. Oudar, D. S. Chemla, *J. Chem. Phys.* **1977**, *66*, 2664. b) J. Zyss, J. L. Oudar, *Phys. Rev. A* **1982**, *26*, 2016.

[30] J. L. Brédas, F. Meyers, B. M. Pierce, J. Zyss, *J. Am. Chem. Soc.* **1992**, *114*, 4928.

  1616-301X/02/0202-0115 $ 17.50+.50/0

[31] G. Bublitz, S. G. Boxer, *Annu. Rev. Phys. Chem.* **1997**, *48*, 213.
[32] G. U. Bublitz, R. Ortiz, S. R. Marder, S. G. Boxer, *J. Am. Chem. Soc.* **1997**, *119*, 3365.
[33] L. Karki, F. W. Vance, J. T. Hupp, S. M. LeCours, M. J. Therien, *J. Am. Chem. Soc.* **1998**, *120*, 2606.
[34] S. Barlow, H. E. Bunting, C. Ringham, J. C. Green, G. U. Bublitz, S. G. Boxer, J. W. Perry, S. R. Marder, *J. Am. Chem. Soc.* **1999**, *121*, 3715.
[35] a) F. W. Vance, L. Karki, J. K. Reigle, J. T. Hupp, M. A. Ratner, *J. Phys. Chem. A* **1998**, *102*, 8320. b) G. U. Bublitz, W. M. Laidlaw, R. G. Denning, S. G. Boxer, *J. Am. Chem. Soc.* **1998**, *120*, 6068. c) F. W. Vance, J. T. Hupp, *J. Am. Chem. Soc.* **1999**, *121*, 4047.
[36] The ring planes are defined as follows: pyridyl N1/C7/C8/C9/C10/C11; phenylene C14/C15/C16/C17/C18/C19; phenyl C1/C2/C3/C4/C5/C6.
[37] B. J. Coe, J. A. Harris, T. Gelbrich, M. B. Hursthouse, *Acta Crystallogr., Sect. C: Cryst. Struct. Commun.* **2000**, *56*, 1487.
[38] L.-T. Cheng, W. Tam, S. H. Stevenson, G. R. Meredith, G. Rikken, S. R. Marder, *J. Phys. Chem.* **1991**, *95*, 10631.
[39] J. Zyss, J. L. Oudar, *Phys. Rev. A* **1982**, *26*, 2028.
[40] See for example: a) M. J. Crossley, S. Gorjian, S. Sternhell, K. M. Tansey, *Aust. J. Chem.* **1994**, *47*, 723. b) C. M. Hudson, R. A. Shenoy, M. E. Neubert, R. G. Petschek, *Liq. Cryst.* **1999**, *26*, 241.
[41] Collect: Data collection software, R. Hooft, Nonius B.V., Delft, The Netherlands **1998**.
[42] Z. Otwinowski, W. Minor, *Methods in Enzymology*, Vol. 276, *Macromolecular Crystallography, Part A* (Eds: C. W. Carter, Jr., R. M. Sweet), Academic, New York **1997**, p. 307.
[43] a) R. H. Blessing, *Acta Crystallogr., Sect. A: Cryst. Phys., Diffr., Theor. Gen. Crystallogr.* **1995**, *51*, 33. b) R. H. Blessing, *J. Appl. Crystallogr.* **1997**, *30*, 421.
[44] G. M. Sheldrick, SHELXL 97, Program for crystal structure refinement, University of Göttingen, Germany **1997**.
[45] L. Karki, J. T. Hupp, *Inorg. Chem.* **1997**, *36*, 3318.
[46] W. Liptay, in *Excited States* (Ed: E. C. Lim), Academic, New York **1974**.
[47] S. K. Kurtz, T. T. Perry, *J. Appl. Phys.* **1968**, *39*, 3798.

  1616-301X/02/0202-0116 $ 17.50+.50/0